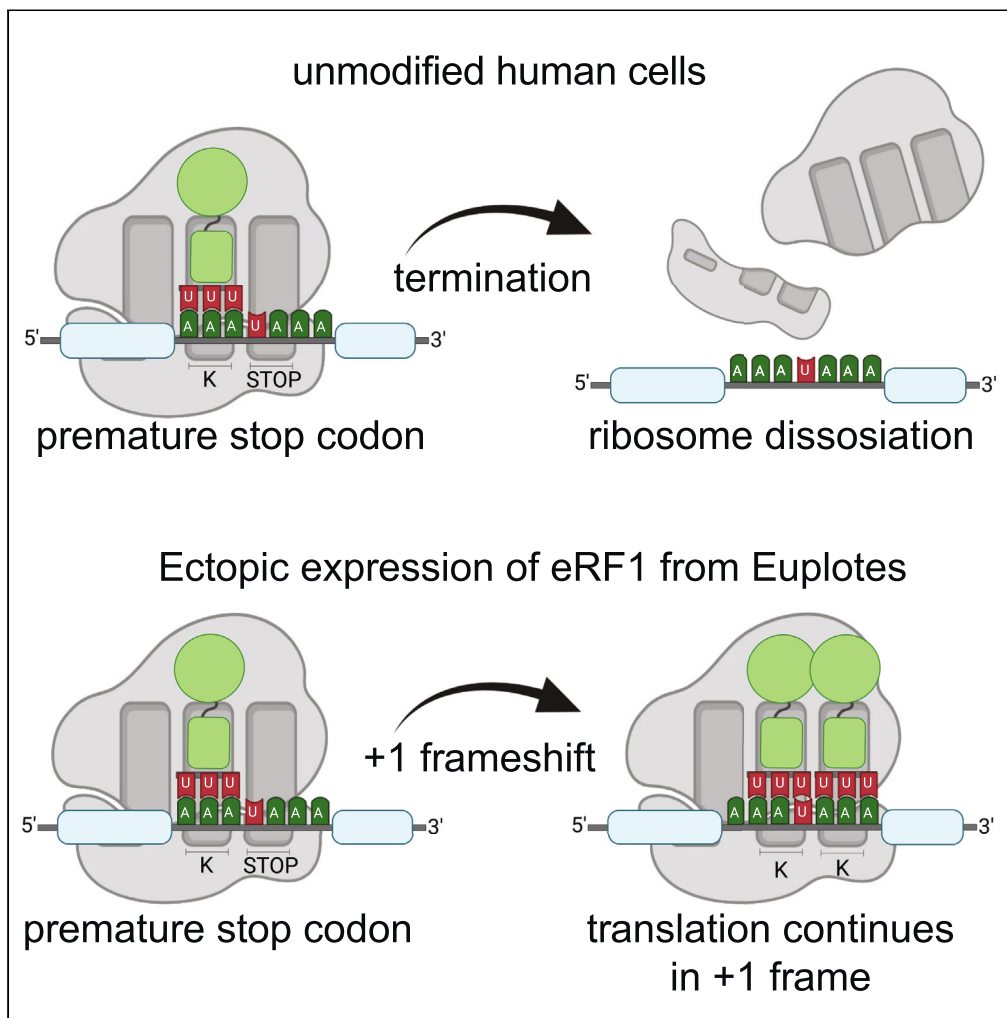


## Article

Eukaryotic release factor 1 from *Euplotes* promotes frameshifting at premature stop codons in human cells

Bozhidar-Adrian Stefanov, Elvis Ajuh, Sarah Allen, Mariusz Nowacki

mariusz.nowacki@unibe.ch

#### Highlights

Ectopic expression of *Euplotes* eRF1 in human cells increases frameshifting rate

The N-terminal domain of *Euplotes* eRF1 is essential for frameshifting induction

Increased frameshifting at a Tay-Sachs disease causative frameshift-stop sequence

Full-length GATA3 protein translation in MCF-7 breast cancer model

Stefanov et al., *iScience* 27, 109413  
April 19, 2024 © 2024 The Author(s).  
<https://doi.org/10.1016/j.isci.2024.109413>

## Article

## Eukaryotic release factor 1 from Euplotes promotes frameshifting at premature stop codons in human cells

Bozhidar-Adrian Stefanov,<sup>1</sup> Elvis Ajuh,<sup>1</sup> Sarah Allen,<sup>1</sup> and Mariusz Nowacki<sup>1,2,\*</sup>

## SUMMARY

Human physiology is highly susceptible to frameshift mutations within coding regions, and many hereditary diseases and cancers are caused by such indels. Presently, therapeutic options to counteract them are limited and, in the case of direct genome editing, risky. Here, we show that release factor 1 (eRF1) from Euplotes, an aquatic protist known for frequent +1 frameshifts in its coding regions, can enhance +1 ribosomal frameshifting at slippery heptameric sequences in human cells without an apparent requirement for an mRNA secondary structure. We further show an increase in frameshifting rate at the premature termination sequence found in the HEXA gene of Tay-Sachs disease patients, or a breast cancer cell line that harbors a tumor-driving frameshift mutation in GATA3. Although the overall increase in frameshifting would need further improvement for clinical applications, our results underscore the potential of exogenous factors, such as Eu eRF1, to increase frameshifting in human cells.

## INTRODUCTION

Programmed ribosomal frameshifting (PRF) is a form of genome expansion through translational recoding. It represents a shift to a different reading frame after a slowdown or a pause of the translating ribosome.<sup>1</sup> PRFs are usually found in organisms with compact genetic information, such as viruses, where precise regulation of protein stoichiometry is essential. While the exact mechanisms of PRFs remain elusive, usually a slippery heptameric mRNA sequence is followed by a secondary structure. Such stem loops<sup>2</sup> or pseudoknots can lodge into the ribosomal mRNA channel, thereby providing the energy necessary for the ribosomal frameshift, as exemplified in the SARS-CoV2 coronavirus.<sup>3</sup>

In contrast to viruses, organisms without genomic size constraints rarely employ PRFs. Additionally, reading frame maintenance is important for prevention of toxic translational products, leading to the evolutionary establishment of efficient translational quality control,<sup>4</sup> and an eRF1 that strongly recognizes stop-codons and ribosomal slowdowns<sup>5</sup> to prevent frameshifting in eukaryotes. Downregulation of eRF1 has been shown as beneficial for the replication of HIV-1, as it increases frameshifting.<sup>2</sup> Most of the few known eukaryotic PRFs are associated with a slippery heptameric sequence<sup>6</sup> that contain a rare tRNA triplet. This causes a translational slowdown that promotes the use of an abundant tRNA complementary to an alternative frame.<sup>7</sup> Another eukaryotic PRF mechanism involves polyamine binding to the ribosome<sup>8</sup> or miRNA control of secondary mRNA structure formation.<sup>9</sup> However, most frameshifting sequences in eukaryotes result from erroneous indel mutations and have implications in hereditary diseases<sup>10</sup> or malignancies, particularly when affecting tumor suppressors.<sup>11</sup>

Strikingly, there are also eukaryotic species, which employ PRFs at a large scale throughout their genomes. This is specifically the case at premature stop codons in organisms from the genome Euplotes. These protists are mostly free-living aquatic ciliates and among the first in which programmed ribosomal frameshifts (PRFs) were described. The early reports of a PRF encoded La motif protein<sup>12</sup> and various kinases<sup>13</sup> were followed by the discovery that different Euplotes species have accumulated numerous frameshift sites over the course of evolution,<sup>14</sup> accounting for more than 10% of their genes.<sup>15–17</sup> While the fitness benefits of such frameshift rich genomes remain unknown, the accumulation of PRF sites suggests a lack of purifying selection, enabling neutral evolution.<sup>18</sup> Ribosome profiling data suggests the presence of both +1 and +2 frameshifts, and that multiple frameshift sites can be found at stop codons within a single ORF.<sup>19</sup> These findings underscore previous results that canonical stop-codons are context dependent in certain organisms<sup>20</sup> and that in Euplotes, a canonical stop codon is recognized as a frameshift site except at the 3'-mRNA-ends.<sup>18</sup>

The molecular basis for these stop-codon reassignments lies in alterations to the N-terminal domain of eRF1 that change UGA from stop to cysteine.<sup>21,22</sup> These modifications simultaneously decrease the affinity for UAG and UAA,<sup>23</sup> causing ribosomal slowdown and increasing the probability of frameshifting.<sup>24</sup> Modifications of the human eRF1 in the y-c-f and the NIKS motifs in the N-terminal domain resulted in ciliate like unipotent stop codon recognition.<sup>25,26</sup> Similar results were found for N-terminal chimeras of human and ciliate eRF1,<sup>24</sup> but not for catalytically dead eRF1.<sup>5</sup> Consequently, it is reasonable to assume that stop-codon reassignment-associated modifications form the mechanistic basis for

<sup>1</sup>Institute of Cell Biology, University of Bern, Baltzerstrasse 4, 3012 Bern, Switzerland

<sup>2</sup>Lead contact

\*Correspondence: [mariusz.nowacki@unibe.ch](mailto:mariusz.nowacki@unibe.ch)

<https://doi.org/10.1016/j.isci.2024.109413>



the observed tolerance for frameshifts at canonical premature stop codons. Given the high evolutionary conservation of the translational machinery, we explored whether eRF1 and other components from *Euplotes* could have retained function in human cells.

Here, we show that eRF1 from *Euplotes aediculatus* enhances frameshifting at premature stop codons in human cells, as measured by various dual-luciferase and dual-fluorescence reporter vectors. Additionally, we demonstrate that eRF1 increases the intracellular levels of proteins containing an internal frameshift within their coding regions. These findings demonstrate a feasibility in potential therapeutic settings. Gene therapy forms a major pillar of personalized medicine, and it is likely to see an expansion of its clinical uses,<sup>27</sup> especially in the cases of untreatable and severe diseases.

## RESULTS

### Ectopic vector delivery for expression of eRF1 from *Euplotes* in human cells increases frameshifting rate

Eukaryotic translation termination is a meticulously orchestrated process, that involves precise timing of multiple components. Based on the efficient frameshifting at premature stop codons (PTCs) in *Euplotes*, we investigated whether its translation termination components could increase frameshifting in human cells at shifty stop codons (Figure 1A). Alongside the two homologs eRF1a and eRF1b, we also included the eRF1 binding GTPase eRF3, and a tRNA<sup>Lys</sup><sub>UUU</sub> from *Euplotes*, considering their possible involvement in promotion of translation in the +1 frame. To assay the selected components, we employed a dual-luciferase reporter vector containing the most common heptanucleotide (AAA-UAA-A) +1 frameshift sequence of *Euplotes*<sup>19</sup> as a spacer between Renilla Luciferase (RLuc) and a firefly luciferase (FLuc). The highest increase of frameshifting rate, as indicated by the increase in FLuc to RLuc ratio, was measured in cells transfected with eRF1a (Figure 1B), which we used for all further experiments. To validate the finding, we used a T7 rabbit reticulocyte lysate system, which we first pre-incubated with a vector encoding Eu eRF1 for either 5 min or 30 min, before introducing the RLuc/FLuc reporter vector. Notably, the 30 min pre-incubation that results in higher Eu eRF1 levels, led to a greater increase in frameshifting compared to the 5 min pre-incubation (Figure 1C), underscoring the influence of eRF1 levels on frameshifting rate. Next, to exclude potential artifacts caused by transient transfection, we stably integrated Eu eRF1 into human cells and measured frameshifting rates using the RLuc/FLuc reporter (Figure 1D). Additionally, to rule out an effect of the reporter gene sequences itself, we exchanged the RLuc/FLuc pair for NanoLuciferase (NLuc) and its temperature stable variant ThermoLuciferase<sup>28</sup> (TLuc) (Figure 1E) or the FLuc/NLuc dual-luciferase pair (Figure 1G) and observed comparable increase in frameshifting in all reporter constructs. (Figures 1F and 1H) Taken together, these results support the notion that Eu eRF1 elevates frameshifting rates in human cells at the consensus stop-frameshift heptamer sequence from *Euplotes* without the necessity of a secondary structure.

### *Euplotes* eRF1 augments frameshifting in a fluorescent protein reporter vector

To measure frameshifting using a different type of reporter vector, we employed eGFP and tdTomato, interspaced by the consensus heptameric stop-frameshift site from *Euplotes* (Figure 2A). Transfection of this reporter vector into wild type and eRF1 expressing cells revealed tdTomato fluorescence predominantly in the eRF1 cells (Figure 2B). Subsequent western blot analysis unveiled a distinct protein band at 81.2 kDa, corresponding to the expected GFP-tdTomato fusion protein as a frameshift product in the lysates from the eRF1 expressing cells (Figure 2C). Next, instead of the consensus *Euplotes* sequence, we introduced various disease-derived frameshift sites (Figure 2D) as the heptameric spacer between the coding sequences of the two fluorescent proteins. Western blot analysis of these constructs revealed varied amounts of the frameshifted eGFP-tdTomato fusion product (Figure 2E). Notably, in the tested stop-frameshift sequences, Eu eRF1 expressing cells exhibited higher amounts of the fusion protein product compared to the wild type empty vector transfected cells, although both groups were transfected with the same transfection mixture and at the same cell density. This observation suggests that both the heptameric slippery sequence and the ectopic expression of eRF1 are influencing the frameshifting rate.

### Impaired stop-codon recognition is necessary for frameshifting induction by eRF1

Previous research in *Euplotes* suggested that the frameshifting promoting activity of eRF1 stems from its reduced recognition of stop codons.<sup>23</sup> Since stop codon recognition is rooted in conserved motifs within the N-terminal domain of eRF1, we engineered a chimeric eRF1 by fusing this part of *Euplotes* eRF1 to human eRF1. Using the RLuc/FLuc dual-luciferase reporter vector, we confirmed that ectopic expression of this chimeric protein indeed elevated the frameshifting rate similarly to wild type *Euplotes* eRF1 (Figures 3A and 3B). To further validate the significance of the N-terminal domain for frameshifting, we used a mutant version of *Euplotes* eRF1 from *Euplotes*, wherein the TEASIKS motif was replaced with the canonical human TASNIKS. Notably, transfection of this mutant protein did not induce an increase in frameshifting from the RLuc/FLuc reporter as compared to mock transfected cells (Figures 3A and 3B). Subsequent testing of the mutant TASNIKS *Euplotes* eRF1 in an *in-vitro* translation reaction using the T7 rabbit reticulocyte system revealed only a minor increase in frameshifting (Figure 3C). To further strengthen the hypothesis that robust stop codon recognition is required for frameshifting prevention, we used siRNA to reduce the levels of endogenous eRF1 (Figure 3D). Upon testing with the RLuc/FLuc reporter, we found an increase of frameshifting compared to the scramble RNA treated control, and an even more pronounced increase when siRNA was combined with *Euplotes* eRF1 (Figure 3E). Combined, these findings suggest that impaired stop-codon recognition is the underlying cause of *Euplotes* eRF1 frameshift inducing function.

### *Euplotes* eRF1 increases the expression of full-length proteins with internal frameshift-stop mutations

Since frameshifting in biological systems would affect a single protein, we aimed to test the applicability of eRF1 with reporter genes containing a frameshift mutation in the middle of their coding sequence. ThermoLuciferase (TLuc) has a natural internal Lys-Lys site, which we

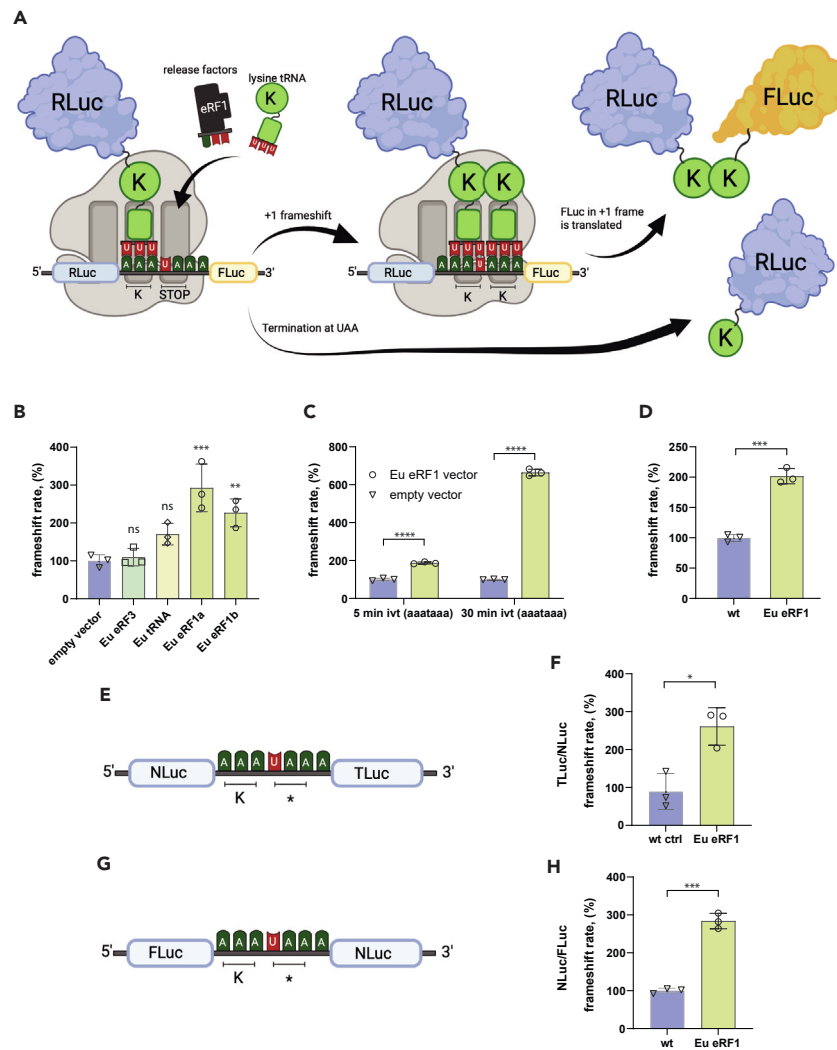


**Figure 1. Ectopic expression of eRF1 from Euplotes in human cells increases frameshifting rate**

(A) Schematic depiction of a dual-luciferase reporter mRNA containing an AAAUAAA frameshift site interspersing RLuc and FLuc reporter genes with translating ribosomes attached to the sequence. Termination at UAA results in RLuc production, while +1 frameshift yields an RLuc-KK-FLuc fusion protein.

(B) Co-transfection of translation termination machinery from Euplotes and a RLuc-frameshift-FLuc into human cells. Frameshifting percentage corresponds to the FLuc/RLuc over the empty vector control FLuc/RLuc rate. Bar plot shows mean  $\pm$  SD of n = 3 replicates shown as individual data points.

(C) *In vitro* (ivt) frameshifting assay using the RLuc-frameshift-FLuc reporter. Incubation time indicate pre-incubation with Eu eRF1 encoding vector. Bar plot shows mean  $\pm$  SD of n = 3 replicates shown as individual data points.

(D) Frameshifting of RLuc-frameshift-FLuc reporter into human cells with stably integrated Eu eRF1. Bar plot shows mean  $\pm$  SD of n = 3 replicates shown as individual data points.

(E) Schematic depiction of a dual-luciferase reporter mRNA containing a AAAUAAA frameshift site interspersing NLuc and TLuc reporter genes.

(F) Frameshifting of NLuc-frameshift-TLuc reporter into human cells with stably integrated Eu eRF1. Bar plot shows mean  $\pm$  SD of n = 3 replicates shown as individual data points.

(G) Schematic depiction of a dual-luciferase reporter mRNA containing a AAAUAAA frameshift site interspersing FLuc and NLuc reporter genes.

(H) Frameshifting of FLuc-frameshift-NLuc reporter into human cells with stably integrated Eu eRF1. Bar plot shows mean  $\pm$  SD of n = 3 replicates shown as individual data points.

Statistical analysis was conducted using a two-tailed t-test for C, D, F, H, and a one-way ANOVA based multiple comparisons of the groups to the empty vector control group for b). ns: not significant, \*p < 0.05, \*\*p < 0.01, \*\*\*p < 0.001, \*\*\*\*p < 0.0001.

modified to AAA-TAA-A (Figure 4A), and delivered this reporter gene both in wild type and Euplotes eRF1 transfected cells. The measured luminescence signal, which we normalized to a non-shifted reporter, was stronger in the Eu eRF1 cells (Figure 4B). Recognising that read-through suppression or frameshifting at actual 3' stop codons can potentially be harmful, we employed a TLuc reporter vector with a frameshift Lys-Lys site near the C-terminus of the protein (Figure 4C). In this case, no increase in luminescence was observed in the eRF1 modified

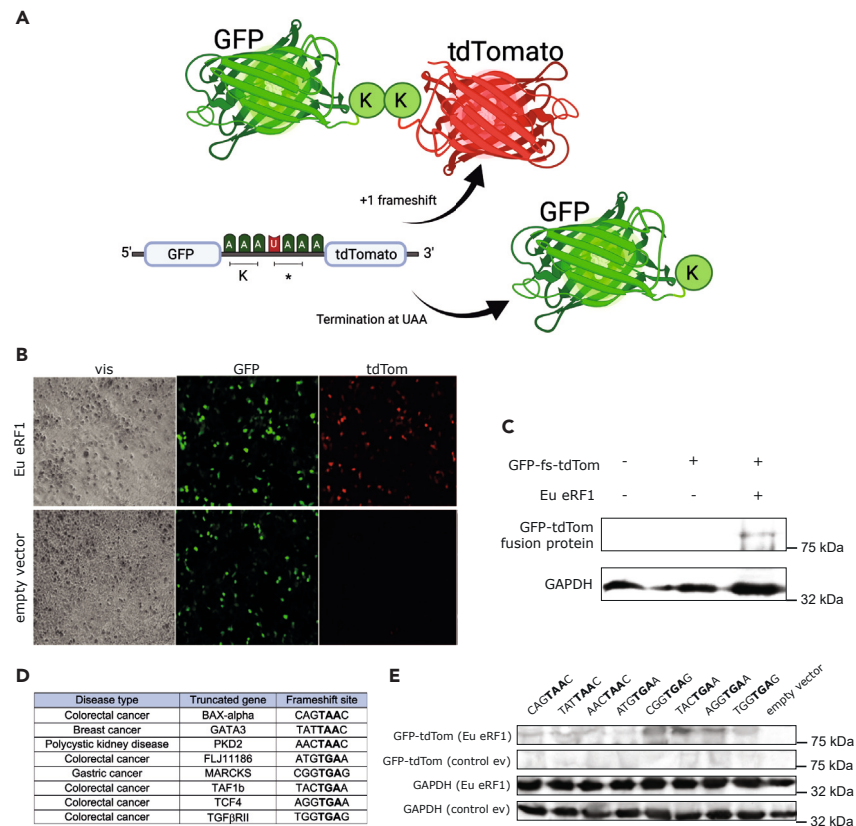


**Figure 2. Euplotes eRF1 increases the frameshifting rate for dual fluorescence reporters**

(A) Schematic depiction of a dual-fluorescence reporter containing an AAAUAAA frameshift site interspacing GFP and tdTomato reporter genes. Termination at UAA results in GFP production, while +1 frameshift yields an GFP-KK-tdTomato fusion protein.

(B) Microscopic visualization of human cells transfected with a dual-fluorescence reporter encoding for GFP-frameshift-tdTomato and either an empty or eRF1 encoding vector.

(C) Western blot analysis of untransfected, transfected with only a dual fluorescence reporter vector, or with the reporter vector and an Eu eRF1 encoding vector.

(D) An excerpt of human disease-causing stop-frameshift mutation heptameric sequences.

(E) Western blot analysis of human cells transfected with either empty vector or an Eu eRF1 encoding vector, and co-transfected with either empty vector or dual-fluorescence vectors encoding for GFP and tdTomato interspaced by human disease-derived heptameric sequences.

cells compared to the wild type (Figure 4D). To explore the potential of eRF1 for increasing the full-length expression of disease associated proteins, we used hexosaminidase A (HexA) as a test model. This is a developmentally essential enzyme and frameshift truncations are causative of the Tay-Sachs disease. First, we introduced a heptameric premature stop codon sequence from a mutant HEXA variant (1278insTATC<sup>29</sup>) between RLuc and FLuc (Figure 4E). Using this reporter, we detected an increase of frameshifting in comparison to empty vector in our established *in vitro* T7 reticulocyte assay (Figure 4F) demonstrating the potential feasibility of the approach. Subsequently, we used Tay-Sachs patient-derived fibroblasts and measured the enzyme activity both in wild type and Euplotes eRF1 transfected cells. Notably, a minor, but statistically significant increase ( $p = 0,02$ ) in the enzymatic activity was measured in the Eu eRF1 transfected cells compared to the wild type (Figure 4G). Overall, these results demonstrate the potential applicability of Euplotes eRF1 for personalized gene therapies, particularly in cases where a premature stop codon is coupled to a frameshift, and a minor increase of full-length protein levels may provide therapeutic benefits.

### Full length Gata3 translation is promoted by Eu eRF1 in a breast cancer model

Indel mutations leading to frameshifts in the GATA3 mRNA stand out as pivotal drivers of breast cancer development and progression.<sup>30</sup> The MCF7 cell line is a primary tumor line derived from an invasive breast ductal carcinoma and harbors a naturally occurring monoallelic truncation in GATA3 (Figure 5A). We sought to determine if ectopic expression of Euplotes eRF1 can increase the amounts of full length Gata3 protein. First, we stably integrated Eu eRF1 into the genome and selected monoclonal cell populations, which were tested for expression of Euplotes eRF1 (Figure 5B). Sub-line Nr.6 exhibited the highest Eu eRF1 expression and was subjected to western blot analysis for Gata3 expression. Using an antibody that recognizes the N-terminus of the protein, we were able to detect both the truncated and

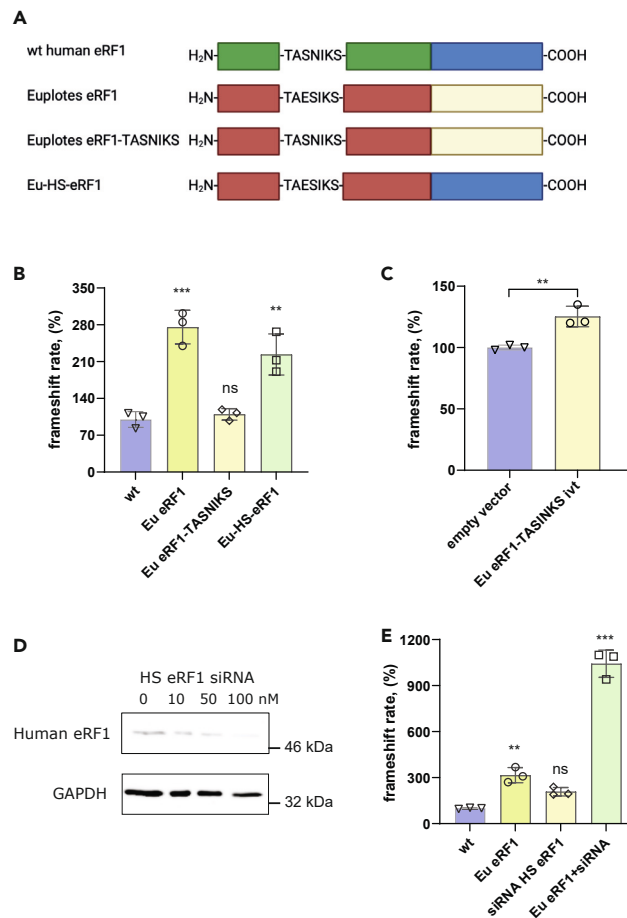


**Figure 3. Decreased stop-codon recognition is necessary for frameshifting induction by eRF1**

(A) Schematic representation of wild type human eRF1, Euplotes eRF1, a chimeric construct in which the TAESIKS motif in eRF1 from Euplotes was replaced with the TASNIKS motif from human eRF1 and a chimeric protein in which the whole N-terminal domain from Euplotes was fused to the C-terminal domain of human eRF1.

(B) Frameshifting of RLuc-frameshift-FLuc reporter in human cells co-transfected with empty vector (wt), Eu eRF1, a mutant Eu eRF1-TASNIKS, and a chimeric Eu-HS-eRF1 containing the N-term domain of Eu eRF1. Bar plot shows mean  $\pm$  SD of n = 3 replicates shown as individual data points.

(C) *In vitro* frameshifting assay using an RLuc-frameshift-FLuc reporter in a reaction pre-incubated for 30 min with either an empty or Eu eRF1-TASNIKS encoding vector. Bar plot shows mean  $\pm$  SD of n = 3 replicates shown as individual data points.

(D) Western blot analysis of human cells transfected with various concentrations of siRNA targeting human eRF1.

(E) Frameshifting of RLuc-frameshift-FLuc reporter in human cells co-transfected with empty vector (wt), Eu eRF1, siRNA targeting human eRF1, Eu eRF1 and siRNA (100 nM) targeting human eRF1. Bar plot shows mean  $\pm$  SD of n = 3 replicates shown as individual data points.

Statistical analysis was conducted using a two-tailed t-test for (C) and a one-way ANOVA based multiple comparisons of the groups to the control group for (B) and (E). ns not significant, \*p < 0.05, \*\*p < 0.01, \*\*\*p < 0.001.

the full-length protein. Compared to the control cells, we observed an increased full length Gata3 in the eRF1 expressing cells (Figure 5C). It's noteworthy that the detected full-length Gata3 protein was less abundant than the truncated in the wild type cell line, which is unexpected for a heterozygous mutant. However, this is consistent with previous reports suggesting an increased stability of the truncated protein.<sup>30</sup> Interestingly, we observed that sub-line 6 is growing slower than the parental wild type line (Figure 5D), however this effect was not due to reduced viability (Figure 5E) suggesting that Eu eRF1 expression decreases the cell division rate of the MCF7 cells. While further investigation would be necessary to uncover any connection of the slower growth rate to the restoration of full-length Gata3, our results demonstrate the feasibility for using a genetically encoded component to elevate the levels of a frameshift-PTC truncated endogenous protein. Such frameshift-PTC mutations are also prevalent in other tumor suppressor genes and their restoration could unveil an anti-proliferative approach in cancer therapy. Direct killing of cancer cells produces debris that triggers the release of pro-inflammatory and growth stimulatory cytokines that can counteract the therapy,<sup>31</sup> therefore growth suppression is currently viewed as an essential addition for advancing the field.

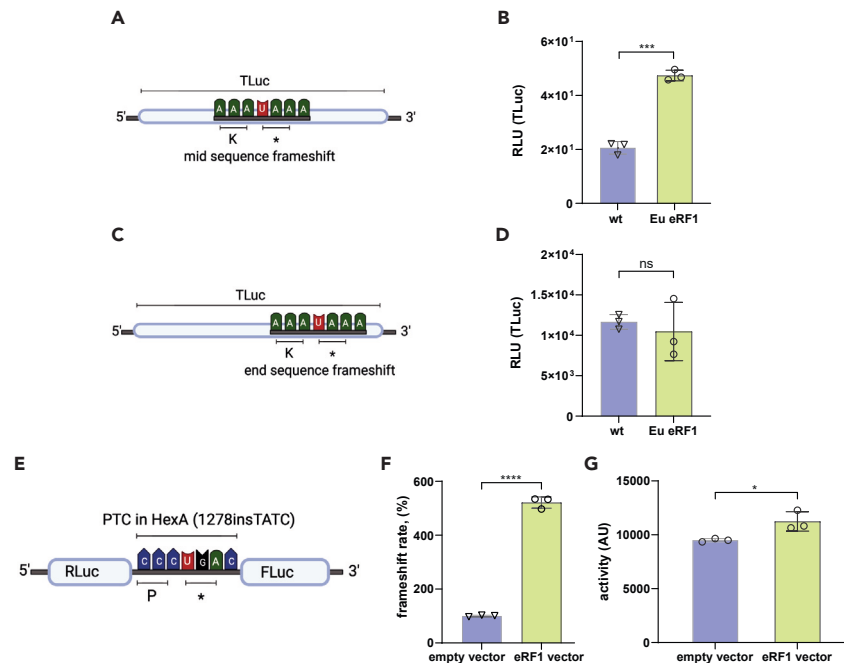


**Figure 4. Euplotes eRF1 increases the expression of full-length proteins encoded with a premature stop-frameshift mutation**

(A) Schematic depiction of a TLuc encoding RNA containing a AAAUAAA frameshift site in the middle of the mRNA.

(B) Luminescence measurement of the reporter depicted in (A) from human cells co-transfected with empty vector (wt) or Eu eRF1. Bar plot shows mean  $\pm$  SD of  $n = 3$  replicates shown as individual data points.

(C) Schematic depiction of a TLuc encoding RNA containing a AAAUAAA frameshift site near the end of the coding region.

(D) Luminescence measurement of the reporter depicted in (C) in human cells co-transfected with empty vector (wt) or Eu eRF1. Bar plot shows mean  $\pm$  SD of  $n = 3$  replicates shown as individual data points.

(E) Schematic depiction of a dual-luciferase reporter mRNA containing the premature termination site derived from the mutant HEXA gene (1278insTATC) as PTC site interspersing the RLuc and FLuc reporter genes.

(F) *In vitro* frameshifting assay using an RLuc-frameshift-FLuc reporter in a reaction pre-incubated for 30 min with an Eu eRF1 encoding vector. Bar plot shows mean  $\pm$  SD of  $n = 3$  replicates shown as individual data points.

(G) Cell count normalized HexA-activity from human patient (HEXA 1278insTATC) fibroblasts (GM00502) transfected with empty vector or Eu eRF1. Bar plot shows mean  $\pm$  SD of  $n = 3$  replicates shown as individual data points.

Statistical analysis was conducted using a two-tailed t-test. *ns*: not significant, \* $p < 0.05$ , \*\* $p < 0.01$ , \*\*\* $p < 0.001$ .

## DISCUSSION

Indel mutations that introduce frameshifts represent a widespread cause of hereditary human diseases, and establishing an efficient genetically encoded system to counteract frameshift mutations hold promise for therapeutic applications across diverse conditions. Currently, personalized gene therapy is envisioned as a next pillar of medicine<sup>27</sup> since such therapies hold the potential to offer remedy in presently untreatable conditions. Therapeutic gene switches can either be introduced *ex vivo* into patient cells<sup>32,33</sup> which are then reimplanted into the host, or delivered directly into tissues.<sup>34</sup> Engineered system can additionally enable unprecedented functions, as evidenced by the signal integration of biological cells with electronic devices<sup>32</sup> for treatment of type 1 diabetes. Notably, such synthetic biology systems use proteins with unprecedented functions, and such proteins can find application in additional areas, such as biopharmaceutical production.<sup>35</sup> Ciliates have long been a source of biological innovation, and the frameshifting tolerance in Euplotes is an excellent example for this. While the delivery of eRF1 from Euplotes in human cells achieved a rather low efficiency of inducible frameshifting, its applicability is potentially still possible for conditions requiring the restoration of low levels of full-length protein for therapeutic benefits. A prominent limitation of this approach is that a frameshift does not always result in an immediate stop codon, therefore eRF1 is not fully applicable to all frameshift associated conditions. Additionally, future work must establish in more detail whether the general translation termination at proper stop codons is affected in human cells. It is known that in ciliates, translation termination is context dependent and relies on 3' UTR sequences and polyA binding proteins<sup>20</sup> as these might favor translation termination.

Previously, Euplotes eRF1 was used in combination with an endogenous frameshifting sequence in yeast, which resulted in higher increase in the frameshifting rate than in our study. This suggests that some sequences are better suited for frameshifting, and a more detailed characterization of all heptameric sites needs to be conducted. Additionally, the mRNA and translation levels might affect the levels of frameshifting rate increase that can be achieved. Nonsense mediated decay (NMD) might reduce the total level of the mRNA significantly and thereby indirectly prevent the induction of a frameshift. Among the additional reasons for higher frameshifting in yeast is the similarity to Euplotes eRF1 of the yeast eRF1.<sup>36</sup> Surprisingly, a chimeric protein containing both human and Euplotes domains did not function better in human cells than the eRF1



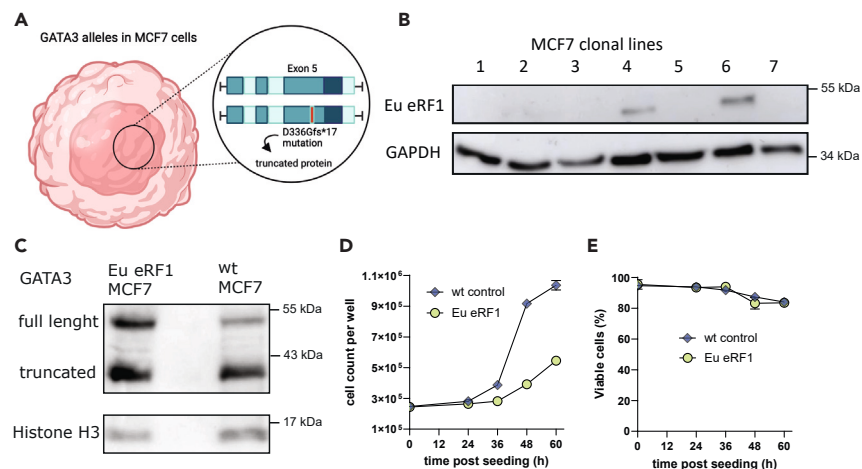


**Figure 5. Full length GATA3 expression is restored in a breast cancer model by Euplotes eRF1**

(A) The pleural effusion derived breast adenocarcinoma cell line MCF7 has a naturally occurring heterozygotic D336Gfs\*17 frameshift mutation. (B) Western blot analysis for Eu eRF1 expression upon stable integration of its expression vector in MCF7 cells. (C) Western blot analysis for GATA3 expression in monoclonal Eu eRF1 line nr.6 and the parental wild type MCF7 line. (D) Cell counts of wild type and Eu eRF1 MCF7 (line nr. 6) cells. Data points show mean  $\pm$  SD of n = 3 replicates. (E) Viability assessment of wild type and Eu eRF1 MCF7 (line nr. 6) cells using trypan blue. Data points show mean  $\pm$  SD of n = 3 replicates.

from Euplotes. Nonetheless, a possible way to increase the efficiency of frameshifting would be to employ a high throughput screening of eRF1 mutagenized variants. Alternatively, screening in combination with other exogenous factors such as suppressor tRNAs, might result in further improvements. Notably, tRNA engineering is providing hope for diseases caused by PTCs mutations<sup>37</sup> and it is likely that such molecules can also be adapted for frameshifting induction. We did show that a tRNA<sup>Lys</sup><sub>UUU</sub> from Euplotes could potentially weakly increase frameshifting (Figure 1B, p = 0.12) either by increasing the decoding efficiency of the +1 frame (AAA) or through its interaction with the ribosome. An interesting future development might also be found in small molecules that promote frameshifting through a decrease of stop codon recognition and increase of frameshift rates through decrease of ribosomal fidelity. Aminoglycoside antibiotics decrease the fidelity of the ribosome and consequently increase the rate of readthrough of stop codons, and some reports demonstrated that gentamycin could induce readthrough frequencies of up to 2% based on the nucleotide sequence of the mRNA.<sup>38</sup> Such pharmacological reduction of eRF1 levels has been applied to PTC diseases in clinical trials<sup>39,40</sup> and next-generation small molecules with reduced side effects for PTC readthrough therapy are currently being developed.<sup>41</sup> Additionally, our results point to a potential small effect through siRNA mediated knockdown of eRF1 (Figure 3D, p = 0.087) on the frameshift rate. This effect was increased in combination with Euplotes eRF1, raising the question whether these two factors counteract each other, or other effects are responsible for this observation. Notably, cellular stressors, such as oxidative stress were shown to increase both the rate of readthrough and frameshifting in yeast<sup>42</sup> and could potentially be repurposed for biomedical applications. Combinatorial strategies, such as combining aminoglycosides with eRF3 degradation, which additionally reduces levels of eRF1, increased readthrough at premature stop codons.<sup>43</sup> Adapting such PTC readthrough approaches for frameshifting might be possible in certain cases. Another therapeutic option may lie in the inhibition of the quality control machinery that prevents frameshifting and readthrough in human cells, as these systems could possibly detect and eliminate frameshift products.<sup>44</sup> Overall, while our results hint at the potential of using Euplotes eRF1, we believe that multiple approaches, including engineered tRNAs and even small molecules, in combination with a more efficient eRF1 mutant variant could advance this ongoing search for treatment of frameshift mutations and prevent the use of direct genomic interventions.

### Limitations of the study

As mentioned above, clinical applications would generally require higher levels of frameshifting to be achieved than what is currently possible using the wild type eRF1 from Euplotes. Additionally, it is important to clarify whether its expression would affect general translation termination or only premature stop codons. We demonstrated that no increase in frameshifting is measurable for a frameshift site near the end of a specific reporter gene transcript. However, it should be considered that finding evidence of readthrough into the 3' UTR is generally challenging, since readthrough peptides are rapidly degraded in human cells. To obtain information about the general situation, it will be necessary to use high throughput methods like mass spectrometry and ribosome profiling to clarify if an increase of 3' readthrough is present for any endogenous transcripts.

### STAR★METHODS

Detailed methods are provided in the online version of this paper and include the following:

- KEY RESOURCES TABLE



- RESOURCE AVAILABILITY
  - Lead contact
  - Materials availability
  - Data and code availability
- EXPERIMENTAL MODEL AND STUDY PARTICIPANT DETAILS
- METHOD DETAILS
  - Cell culture
  - Molecular cloning
  - Transfection of plasmid DNA
  - Luciferase quantification
  - *In vitro* frameshifting assay
  - Euplotes eRF1 stable cell lines
  - Human eRF1 silencing
  - Immunoblotting
- QUANTIFICATION AND STATISTICAL ANALYSIS

## ACKNOWLEDGMENTS

We would like to thank the entire Nowacki Lab for helpful discussions and Nasikhat Stahlberger for technical support. We would like to thank the group of Prof. em. Dr. Matthias Hediger for breast cancer cell line MCF7 and Prof. Oliver Pertz for the HEK293FT cell line.

This research was supported by European Research Council Grants (ERC) 260358 “EPIGENOME” and 681178 “G-EDIT”, Swiss National Science Foundation grants 31003A\_166407 and 31003A\_184680, and grants from the National Center of Competence in Research (NCCR) RNA and Disease.

## AUTHOR CONTRIBUTIONS

The research design was done by B.-A.S., S.A., and M.N., and the experiments were performed by B.-A.S. and E.A. The manuscript was written by B.-A.S. and reviewed by M.N.

## DECLARATION OF INTERESTS

We declare no conflict of interest.

Received: December 7, 2023

Revised: January 23, 2024

Accepted: February 29, 2024

Published: March 4, 2024

## REFERENCES

1. Belcourt, M.F., and Farabaugh, P.J. (1990). Ribosomal frameshifting in the yeast retrotransposon Ty: tRNAs induce slippage on a 7 nucleotide minimal site. *Cell* 62, 339–352. [https://doi.org/10.1016/0092-8674\(90\)90371-k](https://doi.org/10.1016/0092-8674(90)90371-k).
2. Kobayashi, Y., Zhuang, J., Peltz, S., and Dougherty, J. (2010). Identification of a cellular factor that modulates HIV-1 programmed ribosomal frameshifting. *J. Biol. Chem.* 285, 19776–19784. <https://doi.org/10.1074/jbc.M109.085621>.
3. Bhatt, P.R., Scaiola, A., Loughran, G., Leibundgut, M., Kratzel, A., Meurs, R., Dreos, R., O’Connor, K.M., McMillan, A., Bode, J.W., et al. (2021). Structural basis of ribosomal frameshifting during translation of the SARS-CoV-2 RNA genome. *Science* 372, 1306–1313. <https://doi.org/10.1126/science.abf3546>.
4. Simms, C.L., Yan, L.L., Qiu, J.K., and Zaher, H.S. (2019). Ribosome Collisions Result in +1 Frameshifting in the Absence of No-Go Decay. *Cell Rep.* 28, 1679–1689.e4. <https://doi.org/10.1016/j.celrep.2019.07.046>.
5. Yang, Q., Yu, C.-H., Zhao, F., Dang, Y., Wu, C., Xie, P., Sachs, M.S., and Liu, Y. (2019). eRF1 mediates codon usage effects on mRNA translation efficiency through premature termination at rare codons. *Nucleic Acids Res.* 47, 9243–9258. <https://doi.org/10.1093/nar/gkz710>.
6. Baranov, P.V., Wills, N.M., Barriscale, K.A., Firth, A.E., Jud, M.C., Letsou, A., Manning, G., and Atkins, J.F. (2011). Programmed ribosomal frameshifting in the expression of the regulator of intestinal stem cell proliferation, adenomatous polyposis coli (APC). *RNA Biol.* 8, 637–647. <https://doi.org/10.4161/rna.8.4.15395>.
7. Stahl, G., McCarty, G.P., and Farabaugh, P.J. (2002). Ribosome structure: revisiting the connection between translational accuracy and unconventional decoding. *Trends Biochem. Sci.* 27, 178–183. [https://doi.org/10.1016/s0968-0004\(02\)02064-9](https://doi.org/10.1016/s0968-0004(02)02064-9).
8. Matsufuji, S., Matsufuji, T., Miyazaki, Y., Murakami, Y., Atkins, J.F., Gesteland, R.F., and Hayashi, S. (1995). Autoregulatory frameshifting in decoding mammalian ornithine decarboxylase antizyme. *Cell* 80, 51–60. [https://doi.org/10.1016/0092-8674\(95\)90450-6](https://doi.org/10.1016/0092-8674(95)90450-6).
9. Belew, A.T., Meskauskas, A., Musalgaonkar, S., Advani, V.M., Sulima, S.O., Kasprzak, W.K., Shapiro, B.A., and Dinman, J.D. (2014). Ribosomal frameshifting in the CCR5 mRNA is regulated by miRNAs and the NMD pathway. *Nature* 512, 265–269. <https://doi.org/10.1038/nature13429>.
10. Bell, C.J., Dinwiddie, D.L., Miller, N.A., Hateley, S.L., Ganusova, E.E., Mudge, J., Langley, R.J., Zhang, L., Lee, C.C., Schilkey, F.D., et al. (2011). Carrier testing for severe childhood recessive diseases by next-generation sequencing. *Sci. Transl. Med.* 3, 65ra4. <https://doi.org/10.1126/scitranslmed.3001756>.
11. Rampino, N., Yamamoto, H., Ionov, Y., Li, Y., Sawai, H., Reed, J.C., and Perucho, M. (1997). Somatic frameshift mutations in the BAX gene in colon cancers of the microsatellite mutator phenotype. *Science* 275, 967–969. <https://doi.org/10.1126/science.275.5302.967>.

12. Aigner, S., Lingner, J., Goodrich, K.J., Grosshans, C.A., Shevchenko, A., Mann, M., and Cech, T.R. (2000). Euplotes telomerase contains an La motif protein produced by apparent translational frameshifting. *EMBO J.* 19, 6230–6239. <https://doi.org/10.1093/emboj/19.22.6230>.
13. Tan, M., Liang, A., Brünen-Nieweler, C., and Heckmann, K. (2001). Programmed translational frameshifting is likely required for expressions of genes encoding putative nuclear protein kinases of the ciliate *Euplotes octocarinatus*. *J. Eukaryot. Microbiol.* 48, 575–582. <https://doi.org/10.1111/j.1550-7408.2001.tb00193.x>.
14. Möllenbeck, M., Gavin, M.C., and Klobutcher, L.A. (2004). Evolution of programmed ribosomal frameshifting in the TERT genes of *Euplotes*. *J. Mol. Evol.* 58, 701–711. <https://doi.org/10.1007/s00239-004-2592-0>.
15. Klobutcher, L.A. (2005). Sequencing of random *Euplotes crassus* macronuclear genes supports a high frequency of +1 translational frameshifting. *Eukaryot. Cell* 4, 2098–2105. <https://doi.org/10.1128/EC.4.12.2098-2105.2005>.
16. Wang, R., Xiong, J., Wang, W., Miao, W., and Liang, A. (2016). High frequency of +1 programmed ribosomal frameshifting in *Euplotes octocarinatus*. *Sci. Rep.* 6, 21139. <https://doi.org/10.1038/srep21139>.
17. Wang, R., Zhang, Z., Du, J., Fu, Y., and Liang, A. (2016). Large-scale mass spectrometry-based analysis of *Euplotes octocarinatus* supports the high frequency of +1 programmed ribosomal frameshift. *Sci. Rep.* 6, 33020. <https://doi.org/10.1038/srep33020>.
18. Gaydukova, S.A., Moldovan, M.A., Vallesi, A., Heaphy, S.M., Atkins, J.F., Gelfand, M.S., and Baranov, P.V. (2023). Nontriplet feature of genetic code in *Euplotes* ciliates is a result of neutral evolution. *Proc. Natl. Acad. Sci. USA* 120, e2221683120. <https://doi.org/10.1073/pnas.2221683120>.
19. Lobanov, A.V., Heaphy, S.M., Turanov, A.A., Gerashchenko, M.V., Pucciarelli, S., Devaraj, R.R., Xie, F., Petyuk, V.A., Smith, R.D., Klobutcher, L.A., et al. (2017). Position-dependent termination and widespread obligatory frameshifting in *Euplotes* translation. *Nat. Struct. Mol. Biol.* 24, 61–68. <https://doi.org/10.1038/nsmb.3330>.
20. Swart, E.C., Serra, V., Petroni, G., and Nowacki, M. (2016). Genetic Codes with No Dedicated Stop Codon: Context-Dependent Translation Termination. *Cell* 166, 691–702. <https://doi.org/10.1016/j.cell.2016.06.020>.
21. Lekomtsev, S., Kolosov, P., Bidou, L., Frolova, L., Rousset, J.-P., and Kisselev, L. (2007). Different modes of stop codon restriction by the *Stylonychia* and *Paramecium* eRF1 translation termination factors. *Proc. Natl. Acad. Sci. USA* 104, 10824–10829. <https://doi.org/10.1073/pnas.0703887104>.
22. Lozupone, C.A., Knight, R.D., and Landweber, L.F. (2001). The molecular basis of nuclear genetic code change in ciliates. *Curr. Biol.* 11, 65–74. [https://doi.org/10.1016/S0960-9822\(01\)00028-8](https://doi.org/10.1016/S0960-9822(01)00028-8).
23. Klobutcher, L.A., and Farabaugh, P.J. (2002). Shifty ciliates: frequent programmed translational frameshifting in euplotids. *Cell* 111, 763–766. [https://doi.org/10.1016/S0092-8674\(02\)01138-8](https://doi.org/10.1016/S0092-8674(02)01138-8).
24. Vallabhaneni, H., Fan-Minogue, H., Bedwell, D.M., and Farabaugh, P.J. (2009). Connection between stop codon reassignment and frequent use of shifty stop frameshifting. *RNA* 15, 889–897. <https://doi.org/10.1261/rna.1508109>.
25. Seit-Nebi, A., Frolova, L., and Kisselev, L. (2002). Conversion of omnipotent translation termination factor eRF1 into ciliate-like UGA-only unipotent eRF1. *EMBO Rep.* 3, 881–886. <https://doi.org/10.1093/embo-reports/kvf178>.
26. Eliseev, B., Kryuchkova, P., Alkalaeva, E., and Frolova, L. (2011). A single amino acid change of translation termination factor eRF1 switches between bipotent and omnipotent stop-codon specificity. *Nucleic Acids Res.* 39, 599–608. <https://doi.org/10.1093/nar/gkq759>.
27. Stefanov, B.-A., and Fussenegger, M. (2022). Biomarker-driven feedback control of synthetic biology systems for next-generation personalized medicine. *Front. Bioeng. Biotechnol.* 10, 986210. <https://doi.org/10.3389/fbioe.2022.986210>.
28. Stefanov, B.-A., Mansouri, M., Charpin-El Hamri, G., and Fussenegger, M. (2022). Sunlight-Controllable Biopharmaceutical Production for Remote Emergency Supply of Directly Injectable Therapeutic Proteins. *Small* 18, e2202566. <https://doi.org/10.1002/smll.202202566>.
29. Kaback, M., Lim-Steele, J., Dabholkar, D., Brown, D., Levy, N., and Zeiger, K. (1993). Tay-Sachs disease—carrier screening, prenatal diagnosis, and the molecular era. *An international perspective, 1970 to 1993. The International TSD Data Collection Network. JAMA* 270, 2307–2315.
30. Gustin, J.P., Miller, J., Farag, M., Rosen, D.M., Thomas, M., Scharpf, R.B., and Lauring, J. (2017). GATA3 frameshift mutation promotes tumor growth in human luminal breast cancer cells and induces transcriptional changes seen in primary GATA3 mutant breast cancers. *Oncotarget* 8, 103415–103427. <https://doi.org/10.18632/oncotarget.21910>.
31. Sulciner, M.L., Serhan, C.N., Gilligan, M.M., Mudge, D.K., Chang, J., Gartung, A., Lehner, K.A., Bielenberg, D.R., Schmidt, B., Dall, J., et al. (2018). Resolvins suppress tumor growth and enhance cancer therapy. *J. Exp. Med.* 215, 115–140. <https://doi.org/10.1084/jem.20170681>.
32. Stefanov, B.-A., Teixeira, A.P., Mansouri, M., Bertschi, A., Krawczyk, K., Hamri, G.C.-E., Xue, S., and Fussenegger, M. (2021). Genetically Encoded Protein Thermometer Enables Precise Electrothermal Control of Transgene Expression. *Adv. Sci.* 8, e2101813. <https://doi.org/10.1002/advs.202101813>.
33. Bertschi, A., Stefanov, B.-A., Xue, S., Charpin-El Hamri, G., Teixeira, A.P., and Fussenegger, M. (2023). Controlling therapeutic protein expression via inhalation of a butter flavor molecule. *Nucleic Acids Res.* 51, e28. <https://doi.org/10.1093/nar/gkac1256>.
34. Mahameed, M., Xue, S., Stefanov, B.-A., Hamri, G.C.-E., and Fussenegger, M. (2022). Engineering a Rapid Insulin Release System Controlled By Oral Drug Administration. *Adv. Sci.* 9, e2105619. <https://doi.org/10.1002/advs.202105619>.
35. Song, H., Fahrig-Kamarauskaitė, J.R., Matabaro, E., Kaspar, H., Shirran, S.L., Zach, C., Pace, A., Stefanov, B.-A., Naismith, J.H., and Künzler, M. (2020). Substrate Plasticity of a Fungal Peptide  $\alpha$ -N-Methyltransferase. *ACS Chem. Biol.* 15, 1901–1912. <https://doi.org/10.1021/acscchembio.0c00237>.
36. Song, L., Chai, B.F., Wang, W., and Liang, A.H. (2006). Identification of translational release factor eRF1a binding sites on eRF3 in *Euplotes octocarinatus*. *Res. Microbiol.* 157, 842–850. <https://doi.org/10.1016/j.resmic.2006.07.005>.
37. Albers, S., Allen, E.C., Bharti, N., Davyt, M., Joshi, D., Perez-Garcia, C.G., Santos, L., Mukthavaram, R., Delgado-Toscano, M.A., Molina, B., et al. (2023). Engineered tRNAs suppress nonsense mutations in cells and in vivo. *Nature* 618, 842–848. <https://doi.org/10.1038/s41586-023-06133-1>.
38. Floquet, C., Hatin, I., Rousset, J.-P., and Bidou, L. (2012). Statistical analysis of readthrough levels for nonsense mutations in mammalian cells reveals a major determinant of response to gentamicin. *PLoS Genet.* 8, e1002608. <https://doi.org/10.1371/journal.pgen.1002608>.
39. Politano, L., Nigro, G., Nigro, V., Piluso, G., Papparella, S., Paciello, O., and Comi, L.I. (2003). Gentamicin administration in Duchenne patients with premature stop codon. Preliminary results. *Acta Myol.* 22, 15–21.
40. Malik, V., Rodino-Klapac, L.R., Viollet, L., Wall, C., King, W., Al-Dahhak, R., Lewis, S., Shilling, C.J., Kota, J., Serrano-Munuera, C., et al. (2010). Gentamicin-induced readthrough of stop codons in Duchenne muscular dystrophy. *Ann. Neurol.* 67, 771–780. <https://doi.org/10.1002/ana.22024>.
41. Gurzeler, L.-A., Link, M., Ibig, Y., Schmidt, I., Galuba, O., Schoenbett, J., Gasser-Didierlaurant, C., Parker, C.N., Mao, X., Bitsch, F., et al. (2023). Drug-induced eRF1 degradation promotes readthrough and reveals a new branch of ribosome quality control. *Cell Rep.* 42, 113056. <https://doi.org/10.1016/j.celrep.2023.113056>.
42. Gerashchenko, M.V., Lobanov, A.V., and Gladyshev, V.N. (2012). Genome-wide ribosome profiling reveals complex translational regulation in response to oxidative stress. *Proc. Natl. Acad. Sci. USA* 109, 17394–17399. <https://doi.org/10.1073/pnas.1120799109>.
43. Baradaran-Heravi, A., Balgi, A.D., Hosseini-Farahabadi, S., Choi, K., Has, C., and Roberge, M. (2021). Effect of small molecule eRF3 degraders on premature termination codon readthrough. *Nucleic Acids Res.* 49, 3692–3708. <https://doi.org/10.1093/nar/gkab194>.
44. Müller, M.B.D., Kasturi, P., Jayaraj, G.G., and Hartl, F.U. (2023). Mechanisms of readthrough mitigation reveal principles of GCN1-mediated translational quality control. *Cell* 186, 3227–3244.e20. <https://doi.org/10.1016/j.cell.2023.05.035>.

## STAR★METHODS

### KEY RESOURCES TABLE

REAGENT or RESOURCE	SOURCE	IDENTIFIER
<b>Antibodies</b>		
Rabbit polyclonal anti-dtTomato	OriGene Technologies GmbH	Cat# TA150128
mouse monoclonal anti-GAPDH	Santa Cruz Biotechnology Inc	Cat# sc-32233; RRID:AB_627679
rabbit monoclonal anti-Histone H3	Cell Signaling Technology	Cat# 9715s; RRID:AB_331563
mouse monoclonal anti-eRF1	Santa Cruz Biotechnology Inc	Cat# sc-365686; RRID:AB_10843214
mouse monoclonal anti-GATA3	Santa Cruz Biotechnology Inc	Cat# sc-269; RRID:AB_627666
goat anti-mouse IgG-HRP	Santa Cruz Biotechnology Inc	Cat# sc-2005; RRID:AB_631736
goat anti-rabbit IgG-HRP	Santa Cruz Biotechnology Inc	Cat# sc-2004; RRID:AB_631746
<b>Critical commercial assays</b>		
Nano-Glo® Luciferase Assay System	Promega	N1110
Nano-Glo® Dual-Luciferase® Reporter Assay System	Promega	N1610
Dual Luciferase Reporter Assay System	Promega	E1910
TnT coupled rabbit reticulocyte lysate T7	Promega	L4610
<b>Deposited data</b>		
Western blot images	Mendeley data	10.17632/6b6r2788ys.1
<b>Experimental models: Cell lines</b>		
HEK293FT	ATCC	PTA-5077
MCF-7	ATCC	CRL-12584
human patient fibroblasts (HEXA 1278insTATC)	Coriell Institute for Medical Research	GM00502
<b>Oligonucleotides</b>		
eRF1 siRNA 5'-caacaaagacuaaacuuu-3'	Sigma-Aldrich	Custom order
<b>Recombinant DNA</b>		
Synthetic gene fragments	Twist bioscience	Custom order
<b>Software and algorithms</b>		
Prism GraphPad 10	GraphPad Software Inc.	<a href="https://www.graphpad.com">https://www.graphpad.com</a>
Adobe Illustrator CC	Adobe Inc.	<a href="https://www.adobe.com/">https://www.adobe.com/</a>
Biorender	Science Suite Inc.	<a href="https://www.biorender.com">https://www.biorender.com</a>
Benchling	Benchling	<a href="https://www.benchling.com">https://www.benchling.com</a>

## RESOURCE AVAILABILITY

### Lead contact

Communication and requests should be addressed directly to the lead contact Prof. Mariusz Nowacki ([mariusz.nowacki@unibe.ch](mailto:mariusz.nowacki@unibe.ch)).

### Materials availability

Materials used in this study are available from the [lead contact](#) upon reasonable request.

### Data and code availability

- The dataset is publicly available. Western blot images are uploaded to Mendeley data with accession number indicated in the [key resources table](#).
- No original code is reported in this paper.
- Any additional data or information is available from the [lead contact](#) upon reasonable request.

## EXPERIMENTAL MODEL AND STUDY PARTICIPANT DETAILS

In this study, the publicly available human cell lines human kidney embryonic HEK293FT (PTA-5077) and breast carcinoma MCF-7 (CRL-12584) were used as generalisable models for human cells. Both cell lines are derived from female sex. The cultured cells were regularly tested for mycoplasma contaminations using a validated qPCR assay. Additionally, patient derived fibroblasts were used in one experiment (GM00502).

## METHOD DETAILS

### Cell culture

HEK293FT cells (PTA-5077), breast carcinoma cell line MCF7 (CRL-12584) and patient derived fibroblasts (GM00502) were cultured using Dulbecco's modified eagle medium-high glucose (Sigma Aldrich, Switzerland) supplemented with 10% fetal bovine serum (Rockland Immunochemicals, Inc Limerick, PA 19468) and 2 mM L-glutamine (Bioconcept Ltd, Switzerland). The cells were incubated in HERA cell-150 incubator (Thermofisher Scientific, Switzerland) at 37°C with 5% CO<sub>2</sub>.

### Molecular cloning

Standard restriction digestion and ligation was used for cloning of the expression and reporter vectors used in this study. Dual-luminescence or dual-fluorescent vectors contain a heptameric nucleotide sequence between the two proteins encoded by the construct, causing a +1 frameshift to be required for translation of the second protein. Sanger sequencing (Microsynth AG, Switzerland) was used to verify the sequences of all constructs.

### Transfection of plasmid DNA

Cultured cells were transfected with polyethylenimine (Sigma-Aldrich, Switzerland) at a ratio of 3:1 PEI:DNA, or lipofectamine2000 (ThermoFisher Scientific, Switzerland) following the manufacturer's procedures at a ratio of 3:1 lipofectamine 2000:DNA. Briefly, 3 µL lipofectamine2000 was diluted in 100 µL Opti-MEM medium (ThermoFisher Scientific, Switzerland) and incubated for 5 min at room temperature. The diluted lipofectamine2000 was then added to 1 µg of plasmid DNA diluted in 100 µL Opti-MEM medium. The mixture was incubated for 5 min at room temperature and then added directly to the cells at a confluency of about 90%. One day post-transfection the medium was replaced with Dulbecco's modified eagle medium-high glucose (DMEM) containing 10% FBS and 2 mM L-glutamine. For transfections of eRF1, the cells were transfected 2 days before transfection with the reporter vector.

### Luciferase quantification

Rennilla luciferase (RLuc) and Firefly luciferase (FLuc) were quantified using the Dual-Glo Luciferase Assay System (Promega AG, Switzerland) following the manufacturer's instruction. Nanoluciferase (NLuc) and Termoluciferase (TLuc) were quantified as described before<sup>28</sup> using the Nano-Glo Luciferase Assay System (Promega AG, Switzerland) and 30 min 75°C for inactivation of NLuc before TLuc readout. Dual luciferase luminescence from FLuc and NLuc was quantified using the Nano-Glo Dual-Luciferase Reporter Assay System (Promega AG, Switzerland) according to the manufacturer's instructions. Luminescence measurements were conducted using Tecan M1000 (Tecan AG, Switzerland) or SpectraMax L (Molecular devices, Switzerland) luminometers. The frameshifting increase was calculated from the FLuc/RLuc ratio of the sample divided by the average FLuc/RLuc ratio of the control for FLuc/RLuc dual luciferase reporter constructs; or the TLuc/NLuc ratio of sample divided by the average TLuc/NLuc of the control for NLuc/TLuc reporters; and the NLuc/FLuc ratio of sample over the average NLuc/FLuc ratio of the control for FLuc/NLuc reporters.

### In vitro frameshifting assay

In each assay, 1 µg Euplotes eRF1a (or eRF1a-TASNIKS) expression vector or empty vector (control) was added to 40 µL rabbit reticulocyte lysate T7 (Promega AG, Switzerland) according to the manufacturer instructions, and the reaction was filled up to 50 µL with ddH<sub>2</sub>O. The mixture was incubated at 30°C for 5 min or 30mins for expression of Euplotes eRF1. Following this, 1 µg of luciferase reporter plasmid (RLuc-AAATAAA-Fluc, or RLuc-CCCTGAC-FLuc) was added to the mixture and incubated for 1 h. The *in vitro* frameshifting was determined from the measured ratios of luminescence FLuc/RLuc as described above.

### Euplotes eRF1 stable cell lines

The HEK293FT and MCF7 lines stably expressing Euplotes eukaryotic release factor 1a (eRF1a) were generated as follows;  $1.0 \times 10^6$  cells/ml of MCF7 cells were seeded in 10 cm dish and transfected using a ratio of 1:1 plasmid DNA and jetOPTIMUS transfection reagent (Polyplus transfection, France). Briefly, 2 µg Euplotes eRF1 expression plasmid DNA was diluted in 200µL jetOPTIMUS buffer and 2µL jetOPTIMUS reagent (Polyplus transfection, France) was added directly into the diluted DNA and incubated for 10 mins at rt. The mixture was added dropwise to the one-day pre-seeded cells at a confluency of about 90%. The cells and empty vector transfected cells were then continuously cultured antibiotic selection medium until no cells in the control population remained. Monoclonal cell lines were separated by restrictive dilution and tested for eRF1a expression by immunoblotting.

### Human eRF1 silencing

A double stranded human eRF1 siRNA [5'-caacaaagacucaaacuuu-3'] (Sigma-Aldrich, Switzerland) and a double stranded scramble control siRNA (Microsynth AG, Switzerland) were used. The siRNAs were delivered through transfection of HEK293 cells with various final concentrations (1 nM, 10 nM, 50 nM & 100 nM) of the siRNAs. Briefly,  $2.0 \times 10^5$  cell/ml were seeded in 12 well plate and transfected one day post-seeding using Lipofectamine2000 according to manufacturer's procedures. Two days post-transfection, cells were harvested for human eRF1 detection via immunoblotting.

### Immunoblotting

RIPA buffer (50 mM Tris-HCl [pH 8.0], 150 mM NaCl, 1% sodium deoxycholate [NaDOC], 1% Triton X-100, and 0.1% SDS) containing 1× protease inhibitor (Roche) was used for cell lysis. Equal concentration of cell lysate was separated using 12% or 20% SDS-PAGE (AppliChem GmbH, Germany). The gel was run using 1× running buffer (125 mM Tris-base, 960 mM Glycine and 0.5% SDS) at constant 80 V until the marker reached below the stacking gel and then run with constant 120 V until appropriate separation was achieved. 1× transfer buffer (250.4 mM Tris base, 1.92M Glycine) and constant 30 V overnight was used to transfer the protein onto 0.45 μm nitrocellulose blotting membrane (Amersham protran, Germany) using wet transfer. The membrane was washed with distilled water and blocked by incubating in blocking buffer, 1× tris buffer saline-tween-0.2% w/v (TBS-0.2%) (50 mM Tris-HCl pH 7.5, 150 mM NaCl) containing 5% nonfat dry milk powder (Migros, Switzerland) for 1 h at rt. The membrane was incubated for 1 h at rt or overnight in primary antibody dilution in 1× TBS-tween 0.2% w/v containing 5% nonfat dry milk powder in the following ratios: Rabbit polyclonal anti-dTomato-TA150128 (1:5000; OriGene Technologies GmbH), mouse monoclonal anti-GAPDH-sc-32233 (1:200; Santa Cruz Biotechnology Inc, Germany), rabbit monoclonal anti-Histone H3-9715s (1:1000; Cell Signaling Technology, Netherlands), mouse monoclonal anti-eRF1-sc-365686 (1:200; Santa Cruz Biotechnology Inc, Germany) mouse monoclonal anti-GATA3-sc-269 (1:200; Santa Cruz Biotechnology Inc, Germany). The membrane was washed 3 times with TBS-tween 0.2%. Furthermore, the membrane was incubated for 1 h at rt with the following secondary antibodies diluted in 1× TBS-tween 0.2% w/v containing 5% nonfat dry milk powder in the following ratio: Goat anti-mouse IgG-HRP; sc-2005 or goat anti-rabbit IgG-HRP-sc-2004 (1:5000; Santa Cruz Biotechnology Inc, Germany). Next, the membrane was washed 5 times with TBS-tween 0.2% with at least a 5mins interval. The membrane was covered with western HRP substrate-WBLUR0600 (Millipore Corporation, MA) and incubated for less than 1 min before readout. Detection was done with the Amersham Image 600 (GE Health Bio-Sciences AB, Sweden).

### QUANTIFICATION AND STATISTICAL ANALYSIS

The represented data is indicated ± standard deviation. Statistical analysis was performed in Prism GraphPad 10 using unpaired t-tests for comparison of the means of two groups, and one-way ANOVA multiple comparisons for comparing the means of 3 or more groups. Data show representative experiment with three independent biological replicates.